Anonymous Referee #1

General comments:

This study investigates the source of spurious arrivals in ambient noise cross-correlation functions calculated over teleseismic differences. The authors explain that such spurious seismic arrivals can be the result of the interference between seismic phases that have time delays that are 'quasi-stationary', that is, their arrival time difference does not vary strongly with source distance. This effect can occur even if the phases do not share a ray path. The authors use two seismic arrays to demonstrate an example involving the P and PKPab phases. In general, this discussion paper is a very nice contribution that will be of interest to a wide audience. I have a few comments that I believe should be addressed before publication, but these are probably quite minor. I will go through these comments in the order in which they appear in the manuscript.

===================

The authors would like to thank the referee for the careful review and helpful suggestions on the manuscript. We modified the manuscript accordingly. Point-to-point responses are provided below.

===================

Specific comments:

- In my opinion, the introduction section of this manuscript is a bit thin on relevant detail. Currently, the authors focus on describing the construction of empirical Green's functions, and briefly mention some of the applications. They consign the majority of the detail to a citation for a review paper. I think this approach is fine when it comes to the empirical Green's function approach, as it isn't really the point of this paper, but I do think the introduction should be expanded to provide more background on the spurious arrivals instead. More specifically, the line of thinking to explain spurious arrivals followed in this paper has already been introduced by Pham et al. (2018), and yet this study has not been cited throughout the current paper. In my opinion, the work of Pham et al. should be presented in the introduction, as it would allow for a nice progression in scientific thinking: Pham et al. focuses on spurious arrivals that share a common ray path, whereas the current study explains those that do not share a ray path.

Pham, T. -S., Tkalˇ ci´ c, H., Sambridge, M., & Kennett, B. L. N. (2018). Earth's correlation wavefield: Late coda correlation. Geophysical Research Letters, 45, 3035– 3042.

https://doi.org/10.1002/2018GL077244

- Similarly, there should probably be some discussion involving Pham et al. (2018) in section 7.

===================

Reply: The authors recognize that the initial version of Introduction needs to be extended. We thank the review for this comment. We were aware of the work by Pham et al. (2018) that interpreted spurious phases in earthquake coda correlations with the stationary-phase arguments: "all phases identified in the correlation wavefield correspond to differences between seismic arrivals with the same ray parameter and a subset of propagation legs in common". We initially thought that readers would be confused by an introduction on coda wave interferometry, while we only focus on microseism noise correlations. Ambient wavefields are dominated by ballistic waves from oceanic microseism sources (5 to 10 s periods). Coda waves excited by large earthquakes are dominated by high-order modes at longer periods (> 20 s) and corresponding to core-related reverberations. We notice that it has not been pointed out explicitly in existing literatures that at large scale, ambient noise correlations are distinct from earthquake coda correlations. Not mentioning the latter could also be misleading. As suggested by the reviewer, we have modified the Introduction and Conclusion sections. We have also added a new Fig. S5 that demonstrates the difference between microseism correlations and coda correlations.

====================

- This might just be a language issue, but on page 2, line 5 the authors state that there have only been a few noise-derived body wave signals. Whilst body waves are certainly more rare than surface waves, nowadays I don't think you can say there are only a few examples. Some examples that could be cited, including the retrieval of core phases, include but not limited to:

https://doi.org/10.1002/grl.50237

https://doi.org/10.1002/2017GL073230

https://doi.org/10.1093/gji/ggw015

https://doi.org/10.1002/2014GL062198 (Uses the same seismic arrays as the authors)

====================

Reply: The reviewer is correct. It was a typo. We meant fewer compared to surface waves. Several new citations have been added to the Introduction.

====================

- On page 3, the authors describe an interesting kurtosis-based method for discarding noise segments that are contaminated by earthquake signals. Is this the first case of this method being used for processing ambient noise? If so, a little bit more clarity is needed. In particular, the 'expectation operator' needs explaining to avoid confusion. Is it some kind of mean? I think if the equation defining kurtosis is properly explained around page 3 line 5, that would be sufficient detail for this paper.

====================

Reply: To our knowledge, it is the first time that the kurtosis has been applied to noise data processing. The reviewer is right that the expectation here refers to the mean value. We clarify it being "arithmetic mean" in the revision.

====================

- On page 4 line 20, the authors mention 'numerical experiments'. More detail probably needs to be added here. How were these experiments performed? I assume by simulating plane waves passing over the known array geometries, but it is impossible to tell from the current text.

====================

Reply: The referee assumed correctly. We have added some details on the numerical experiments.

"To investigate the resolution capability of the double-array slowness analysis for the FNET-LAPNET geometry, we make numerical experiments by presuming (a) the same slowness at FNET and LAPNET (4.6 s/deg), and (b) different slownesses at FNET (4.7 s/deg) and LAPNET (4.2 s/deg). Assuming plane waves passing through FNET and LAPNET, the time delays between FNET and LAPNET station pairs can be calculated from Eq. (1). The wavelet of the observed spurious phase (5 to 10 s bandpass filtered) is convolved with the time delays to synthesize the correlation functions. The synthesized correlations are beamed by Eq. (2) for various slownesses. The results are plotted in Fig. 6. In both cases, the slownesses of the correlated waves at FNET and LAPNET are well resolved, justifying the reliability of our slowness discrepancy estimation in Fig. 5a."

===================

- Similarly, on page 4 line 20 - 21 the authors quote the simulated slowness values for their numerical experiment, but on the first read it appears as if these values drop out of thin air until it is explained that they match the observed slowness from the real data on line 25. I would suggest that the order of the explanation is changed here so that it is clear that the numerical experiment simulates the observed slowness values.

===================

Reply: We agree that exchanging figs 5 and 6 and relevant text improves readability. Thanks for this suggestion.

===================

- On page 5 lines 5 - 15, the authors explain how they identify the relevant interfering phases. In the current form, the explanation is slightly convoluted and hard to follow. I think it would benefit if the authors explicitly state that the culprits are a P-wave sourced 89 degrees from, and recorded at, FNET, and PKPab sourced 152 degrees from LAPNET. At the moment the arrays at which each phase is recorded is only implied by the text, when it is key to identifying the source region.

===================

Reply: We agree with the proposed clarification and have modified the statement accordingly.

===================

- The authors comment on page 5 line 12 that PcP-PKPab also matches the required time delay. Is this candidate discarded due to an incorrect slowness for PcP? Again it isn't stated, but only implied. Perhaps the PcP slowness should be quoted here too to drive the point home.

===================

Reply: Yes, the slowness comparisons are critical. We have clarified this point and quoted the PcP slowness.

===================

- A minor confusion occurs on page 5 line 17, the authors state that Fig. 6 can be used to located the source responsible, when in reality Fig. 6 only gives you the source distances. Unless I'm mistaken, to actually locate the source you need other information such as the array locations, and whether the source is causal or acausal.

===================

Reply: Fig. 6 provides source-receiver distances. Receiver locations are of course necessary for locating the sources. We have clarified that in the revision.

====================

- The supplementary material is currently just a pile of a couple of figures referred to in the main text. I think the supplementary material should include the information required to stand on its own. I think a couple of sentences explaining each supplemental figure, and its relevance to the main text, are warranted.

====================

Reply: Subheadings and explanatory sentences have been added to Supplementary.

====================

Technical comments: - On page 8 lines 4 - 7 there are a few sentences that don’t make much sense, and are grammatically incorrect. I suggest the authors rewrite these sentences to clarify.

====================

Reply: We have rewritten this part. Thanks for pointing this out.

====================

- In Fig. 4, on the bottom vespagram, ’spurious’ is missing an ’s’.

====================

Reply: Corrected. Thanks.

====================

In conclusion, I believe that in order to provide the clarifications and explanations that I have requested above, it is likely only a minor revision will be required.

Pilar Sánchez Sánchez-Pastor (Referee #2)

psanchez@ictja.csic.es

Received and published: 29 October 2019

This is an interesting manuscript that studies a spurious signal observed in the correlograms of seismic noise between two distant seismic networks. The authors employ the double-beam method to estimate the slowness of several seismic phases as a function of distance and thus, track the observed interfering waves and determine the origin of that spurious signal. Furthermore, the authors provide a physical explanation for such signal through numerical simulations and observe it as well in synthetic correlograms. In my opinion, the study is well addressed and scientifically valuable. However, the presentation of the manuscript should be improved before possible publication. Basically, the manuscript needs to be written with more care and some minor corrections are required. My suggestions and comments are described below.

===================

The authors would like to thank the reviewer for her careful reading and constructive comments. Point-to-point replies are provided below.

===================

- In the Introduction, I would have liked a better introduction of spurious signals, why is useful to study them, mention the previous similar studies and, in general, explain better the problematic. Also, I would update some references with new studies and add some in pag. 2, lines 4-9.

===================

Reply: The authors recognize that the initial version of Introduction needs to be extended. We thank the reviewer for this comment. The other reviewer made a similar comment on the Introduction. We have added new citations and extended the Introduction to better describe the background, especially, some existing applications of noise-derived deep body waves (including spurious phase).

===================

- Line 29, pag. 2: Vague sentence. Some readers very likely would not understand what you mean.

===================

Reply: We agree with the reviewer and have removed this dispensable sentence.

===================

- Line 30, pag. 2: It is worth it to specify the amplitude threshold (how many times of the standard deviation) that you consider to clip the waveforms and avoid large transients.

===================

Reply: We mention in the revision that we clipped at 3.8*std, which is just an empirical choice following previous studies (Poli et al., 2012; Boué et al., 2013). We did not specify the value because the choice is more or less arbitrary. No problem to choose other values. Of course, a very large value (e.g., 100 times) would make the clipping ineffective in removing impulses. A very small value (e.g., 0.1 times) would have a similar effect as the one-bit resampling. A modest choice of 3.8 leads to an effective clipping of large transients and retains the waveform of stationary noise (Fig. 3 for examples).

====================

- Line 5, pag. 3: If it is the first time that the kurtosis is employed in seismic noise processing, the authors should explain it better. For example, the equation described is a comparison between the kurtosis of the distribution under study and the kurtosis of a normal distribution, which is 3.

====================

Reply: Following comments by both reviewers, we have described more on kurtosis, and also explained, as suggested here, that including the term 3 makes the kurtosis of Gaussian distribution zero.

====================

- Line 8, pag. 3: "the segments beyond 1.5 are discarded" why this value? It would be proper a short comment to explain it.

====================

Reply: We have clarified in the revision the threshold of 1.5 is empirical. The threshold, if too small (below ~1), will reject good noise segments, and if too large (above 3-5), will let pass impulsive segments. A value between 1 and 2 is suggested. From our experience, 1.5 works fine for various datasets.

====================

- Line 20, pag. 4: Vague sentence. Which numerical experiments?

====================

Reply: This problem was also raised by the other reviewer. We have described more on the numerical experiments in the revision:

"To investigate the resolution capability of the double-array slowness analysis for the FNET-LAPNET geometry, we make numerical experiments by presuming (a) the same slowness at FNET and LAPNET (4.6 s/deg), and (b) different slownesses at FNET (4.7 s/deg) and LAPNET (4.2 s/deg). Assuming plane waves passing through FNET and LAPNET, the time delays between FNET and LAPNET station pairs can be calculated from Eq. (1). The wavelet of the observed spurious phase (5 to 10 s bandpass filtered) is convolved with the time delays to synthesize the correlation functions. The synthesized correlations are beamed by Eq. (2) for various slownesses."

====================

- Lines 4-9, pag. 5: I think the proposed slowness-track method to identify the ray paths of the interfering waves is not enough clear. In my opinion, this paragraph can be improved and make easier to follow the idea.

- Line 7, pag. 5: "The pairs of seismic phases are rejected if the difference between the distances from the source to the receivers differs from 63 ◦ or if their time delay deviates from 430 s" why? It could be obvious but indicating a reason works out well for a better understanding.

====================

Reply: We agree with these comments and have rephrased this part.

====================

- Line 20, pag. 7: I imagine those results imply a lot of work and they are interesting. So perhaps it is worth adding a supplementary figure.

====================

Reply: See the new Fig. S6 and relevant supplemental text. Thanks for this suggestion.

====================

FIGURES:

- Figure 3: you should use same colours as in Fig 2 to be consistent. Also, the title “after clipping” I would say amplitude clipping or something similar in order to avoid misunderstandings.

====================

Reply: Modified accordingly. Thank you for pointing this out. We ignored this detail.

====================

- Figure 4: The labels a) b) etc are missing. Moreover, you should explain the overlapped signal in the figure caption.

====================

Reply: Labels and text annotation for the beamed signal have been added**.**

====================

- Figure 5: From my point of view, it can be added to the supplementary material. If you consider the supplement is already too long, the Figure S1 is dispensable.

====================

Reply: Thanks for your suggestion. Considering that double-array slowness analysis is first proposed in this paper and the resolution is critical to our argument that the interfering waves have distinct slownesses, and also that SE is an electronic journal that has no constrains on the paper length, we prefer to keep the figure in the main text.

====================

- Figure S1: I would change “removed-mean series” for pre-processed series because you correlate after removing the mean, trend, filtering, whitening... Moreover, I would add in the colored bars at the top a label “i” and in the bars at the bottom “i” and “i-τ” (following the notation of the eq) to illustrate the dislocation applied by the correlation. Although, I believe it is better only correlate the “effective samples” instead of adding zeros. In this way, for large lag times you underestimate the correlation.

====================

Reply: Figure S1 is intended to explain the computation of correlation function in a general sense. The formulae displayed in the figure only require the series being demeaned. So, it is not a problem. Of course, the referee is right in the context of seismograms. The correlation function is routinely calculated by FFT for efficiency. The zero padding at the bottom of Fig. S1 is just for explanatory purpose. Concerning the underestimation of correlation function at large lags, a modified scheme for calculating the correlation function described in figure 2.21 in section 2.4.2 of my thesis can deal with this problem (https://www.theses.fr/2018GREAU023.pdf). This is irrelevant to the topic of this paper. So, we do not talk much on it.

====================

- Figure 8: is it computed or taken from other study?

====================

Reply: All data sources are indicated in the Acknowledgement. We have clarified in the caption that the data in Fig. 8 come from Rascle and Ardhuin (2013).

====================

- Figure 10: you should describe what the red point represents in the figure caption even if this seems obvious. In my view, figure captions should be auto-explicative and if they are not, one should indicate where the reader could find the information.

====================

Reply: We agree that it is common to describe lines and symbols in the caption. But this appears discouraged by Solid Earth. "*A legend should clarify all symbols used and should appear in the figure itself, rather than verbal explanations in the captions (e.g. "dashed line" or "open green circles").*" (https://www.solid-earth.net/for_authors/manuscript_preparation.html) We used text annotations on the figure to indicate that the red dot corresponds to the observed spurious phase beamed at 63° distance.

====================

OTHER MINOR COMMENTS:

- Line 2, pag. 2: "We refer to (Campillo and Roux, 2015)" without parenthesis.

====================

Reply: Corrected. Thanks.

====================

- Lines 26-29, pag. 5: reference?

====================

Reply: Added.

====================

- Line 17-20, pag. 6: Those sentences can be improved.

====================

Reply: We have rephrased this part.

====================

- Line 29, pag. 6: "The ray-based simulation above" would be better like: The above-described ray-based simulation...

- Line 23, pag. 7: In my opinion, this section should be called 'Conclusions'.

====================

Reply: Modified accordingly. Thanks.

===================

Observation and explanation of spurious seismic signals emerging in teleseismic noise correlations

Lei Li[1,2], Pierre Boué[2], Michel Campillo[2]

[1]State Key Laboratory of Earthquake Dynamics, Institute of Geology, CEA, Beijing, China
[2]Université Grenoble Alpes, CNRS, IRD, IFSTTAR, ISTerre, Grenoble, France

Correspondence to: Lei Li (lilei@ies.ac.cn)

Abstract. Deep body waves have been reconstructed from seismic noise correlations in recent studies. Authors prospect their great potentials in deep-Earth imaging. In addition to the expected physical seismic phases, some spurious arrivals having no correspondence in earthquake seismograms are observed from the noise correlations. The origins of the noise-derived body waves have not been well understood. Traditionally, the reconstruction of seismic phases from inter-receiver noise correlations is attributed to the interference between waves from noise sources in the stationary-phase regions. The interfering waves emanating from a stationary-phase location have a common ray path from the source to the first receiver. The correlation operator cancels the common path and extracts a signal corresponding to the inter-receiver ray path. In this study, with seismic noise records from two networks at teleseismic distance, we show that noise-derived spurious seismic signals without correspondence in real seismograms can arise from the interference between waves without common ray path or common slowness. These noise-derived signals cannot be explained by the traditional stationary-phase arguments. Numerical experiments reproduce the observed spurious signals. These signals still emerge for uniformly distributed noise sources, and thus are not caused by localized sources. We interpret the presence of the spurious signals with a less restrictive condition of quasi-stationary phase: providing the time delays between interfering waves from spatially distributed noise sources are close enough, the stack of correlation functions over the distributed sources can still be constructive as an effect of finite frequencies, and thereby noise-derived signals emerge from the source averaging.

1 Introduction

The technique of noise correlation is implemented simply via computation of correlation functions between ambient noise records at receivers. Theoretical and experimental studies (e.g., Lobkis and Weaver, 2001; Wapenaar, 2004) have shown that under restrictive conditions, the inter-receiver correlation function converges toward the response that would be recorded at one receiver if a source was located at the other. This is, by definition, the Green's function of the medium between the two receivers. Great achievements have been realized with the introduction of the noise correlation technique into solid-Earth seismology (Campillo and Paul, 2003; Shapiro and Campillo, 2004). The most common applications are passive imaging (e.g., Sabra et al., 2005; Shapiro et al., 2005) and monitoring (e.g., Brenguier et al., 2008; Wegler et al., 2009) of subsurface using signals derived from seismic noise. We refer to ~~(~~Campillo and Roux~~,~~ (2015) for a systematic review on the recent progress in the theoretical and methodological aspects, and the various noise-based applications.

Both the surface-wave and body-wave parts of the Green's function can be reconstructed from noise correlations. Surface waves are easier to extract due to their dominance in the noise ~~power~~ spectra. There are relatively fewer, yet promising, examples of noise-derived body waves. Some authors have demonstrated that deep body-wave signals that propagate through the mantle and core can be extracted from the correlations of continuous seismograms recorded by seismic networks at regional to global scales (Boué et al., 2013b, 2014; Lin et al., 2013; Nishida, 2013). Several applications followed. For instance, Poli et al. (2015) imaged the core-mantle boundary (CMB) beneath Siberia with P-wave reflections derived from microseisms. Spica et al. (2017) used higher order correlations to retrieve the ScS arrivals and imaged the lateral variations of the CMB beneath Mexico. Besides from ambient noise wavefields excited by ocean waves (Longuet-Higgins, 1950), another strategy to extract the deep body waves relies on the highly coherent late coda waves excited by large earthquakes (Lin and Tsai, 2013; Boué et al., 2014; Xia et al., 2016). The coda-derived deeply incident waves are dominantly related to reflected and refracted core phases (Boué et al., 2014; Phạm et al., 2018). By estimating the differential times between coda-derived core phases, Wang et al. (2015) and Wang and Song (2017) inferred the equatorial anisotropy of the Earth's inner core. The coda correlations contain normal seismic phases as well as spurious phases. A seismic phase is termed normal if it is present in the Green's function of the medium, and spurious if it is not observed in real seismograms and does not obey the theory of seismic wave propagation. Poli et al. (2017) ascribed the vertically traveling ScS-like signals in the vertical-vertical component of coda correlations to the interference of high-order modes that have low attenuations. Using ray theory and stationary-phase arguments, Phạm et al. (2018) interpreted the spurious phases in global coda correlations as results of the interferences between specific ray paths. Tkalčić and Phạm (2018) inferred the shear properties of the Earth's inner core by modelling a spurious phase related to the *J* waves.~~Recently, it has been demonstrated that deep body-wave signals that propagate through the mantle and core can be extracted from ambient noise correlations (e.g., Boué et al., 2013b, 2014; Nishida, 2013). In contrast to previous studies that primarily discussed the reconstruction of normal seismic phases from noise correlations, we focus our analysis here on the interpretation of a spurious seismic phase that can be observed from noise correlations between receivers separated at teleseismic distances. A seismic phase is termed normal if it is present in the Green's function of the medium, and spurious if it is not observed in real seismograms and does not obey the theory of seismic wave propagation.~~

In contrast to the fact that spurious body waves in earthquake coda correlations have been observed and explained, the observation and explanation of spurious phase in ambient noise correlations are lacking yet. In this study, we focus our analysis on the interpretation of a spurious P-type phase that can be observed from the noise correlations between receivers separated at teleseismic distances. This paper is organized as follows. In Sect. 2, we describe the processing of seismic noise data. In Sect. 3, we correlate the processed noise records and show the observation of noise-derived spurious arrivals emerging earlier than the direct P waves. In Sect. 4, we develop a new double-array technique to estimate the slownesses of the interfering waves and analyse the origin of the observed spurious phase. In Sect. 5, we propose a mechanism to explain the generation of the spurious phase. More elaborate numerical experiments are implemented in Sect. 6 to reproduce the observed signals and to investigate the sensitivity to the distribution of seismic noise sources.

2 Noise data processing

Continuous seismograms recorded in 2008 by the broadband stations of the Full Range Seismograph Network of Japan (the FNET array) and the northern Fennoscandia POLENET/LAPNET seismic network in Finland (the LAPNET array), are used in this study to calculate the double-array noise correlations (Fig. 1). The aperture of the LAPNET array is ~700 km, and that of the FNET array is nearly 1,400 km. There are 1,558 FNET-LAPNET station pairs in all. The distance between the FNET and LAPNET stations ranges from ~56° to 70°, with a center~~re~~-to-center~~re~~ distance of 63°.

The processing of seismic noise data is segment-based, as demonstrated in Fig. 2. The processing is similar to that adopted by Poli et al. (2012) and Boué et al. (2013b). First, routine signal-processing operations are applied to the raw seismograms (including mean and linear trend removal, bandpass filtering, 5 Hz down-sampling, instrumental response deconvolution). Then, continuous seismograms are divided into 4-h segments. The frequency spectra of the segments are whitened between periods of 1 s and 100 s. ~~The spectral whitening removes amplitude information and retains only the phase spectrum.~~ One may further clip the spectral-whitened waveform at several times of the standard deviation to reduce large transients~~.~~ (e.g., 3.8 times as in the above-mentioned studies). A selection filter is applied to the segments to detect and reject those containing transient impulses like earthquakes and electronic glitches.

In the previously mentioned studies, the selection filter was based on the energy ratio between segment and daily trace, which can be deemed as a coarse version of the classic STA/LTA method commonly used for earthquake detection (Allen, 1982). Here, we adopt a new kurtosis-based selection filter. The kurtosis, or fourth-order normalized central moment, is defined as $\kappa = \mathbf{E}[s^4]/(\mathbf{E}[s^2])^2 - 3$, with $\mathbf{E}[\cdot]$ the expectation operator for arithmetic mean and s the demeaned waveform. It can be deemed as a measurement of deviation from the Gaussian distribution that has a kurtosis value of zero and is generally expected for stationary ambient seismic noise (Peterson, 1993).~~.~~ The kurtosis~~It~~ is highly sensitive to impulsiveness (Westfall, 2014), close to zero for stationary noise but increasing abruptly in the presence of transient impulses (see Fig. 3 for examples). The selection filter can be applied at any stages of the processing (raw, whitened, clipped waveforms). In this study, segments of kurtosis beyond an empirical threshold of 1.5 are discarded. The kurtosis has also been used in detecting earthquakes and picking phases (e.g., Baillard et al., 2014; Saragiotis et al., 2002) and is first used for noise data processing. Compared to the energy-based selection, the kurtosis-based selection depends on the statistics of the segment itself and is more robust when the strength of seismic noise changes rapidly.

3 Observation of spurious phase

We correlate all of the available pairs of processed noise segments and stack them to produce the correlation function of the year-long data for each FNET-LAPNET station pair. The computation of correlation function is diagrammatized in Fig. S1. The correlation function contains a causal part and an acausal part that correspond to the positive and negative time lags, respectively. In this paper, the acausal correlations correspond to seismic waves that travel from FNET to LAPNET (causal: from LAPNET to FNET).

The noise correlations of all of the FNET-LAPNET station pairs are binned in an inter-station distance interval of 0.1°, to produce the waveform sections for the acausal and causal parts of the noise correlations. The filtered sections (periods of 5 s to 10 s) of the vertical-vertical noise correlations are shown in Fig. 4 and the broadband sections in Fig. S2. The theoretical P and PcP waves marked on the panels are predicted using the Taup program (Crotwell et al., 1999) and the IASP91 Earth model (Kennett and Engdahl, 1991). A coherent arrival between 410 s and 450 s is clearly visible in the acausal section of noise correlations, about 200 s earlier than the direct P wave that should be the primary arrival. The early arrival has no correspondence in the true Green's function of the Earth medium, and thereby is undoubtedly a spurious phase. Spectral analysis indicates that the spurious phase has a peak period of 6.2 s (Fig. S3), typical for secondary microseisms. As estimated from the acausal vespagram in Fig. 4, the emerging time and apparent slowness of the spurious phase at 63° distance are about 430 s and 4.6 s/deg, respectively. The spurious phase is only observed in the vertical-vertical noise correlations, indicating that it is likely a P-type phase. In the causal correlations, a corresponding spurious phase is hardly discriminable.

4 Origin of signals from P-PKPab correlations

In the previous section, a prominent spurious phase was observed in the FNET-LAPNET noise correlations, and its apparent slowness and emerging time were estimated. The double-array configuration offers the possibility to estimate the respective azimuths and magnitudes of the slownesses of the correlated wavefields that should be responsible for the spurious phase. Given a wave with slowness $\boldsymbol{p}^A$ at FNET and a wave with slowness $\boldsymbol{p}^B$ at LAPNET, the time difference between the time delay between the *i*th FNET station and the *j*th LAPNET station and the center-to-center reference time can be determined from Eq. (1):

$$\Delta t_{ij} = \boldsymbol{x}_i^A \cdot \boldsymbol{p}^A - \boldsymbol{x}_j^B \cdot \boldsymbol{p}^B \quad (1)$$

where $\boldsymbol{x}$ are the local coordinates of the station with respect to the array center, and superscripts A and B distinguish between FNET and LAPNET. For a given pair of $(\boldsymbol{p}^A, \boldsymbol{p}^B)$, the noise correlations of all station pairs are beamed by Eq. (2):

$$B(t, \boldsymbol{p}^A, \boldsymbol{p}^B) = \langle\, C_{ij}\big(t + \Delta t_{ij}\big)\rangle \quad (2)$$

Where $\langle\cdot\rangle$ denotes ensemble average and C_{ij} is the correlation function between the ith FNET station and the jth LAPNET station. This delay-and-sum process for the double-array data is known as the double-beam method, which has been applied to earthquake data (e.g., Krüger et al., 1993; Rost and Thomas, 2002) and noise correlations (e.g., Boué et al., 2013a; Roux et al., 2008). Repeating the double-beamforming for a range of $\boldsymbol{p}^A$ and $\boldsymbol{p}^B$, the power map of the double-beamed waveforms $\langle|B(\boldsymbol{p}^A,\boldsymbol{p}^B)|^2\rangle$ provides the optimal slowness estimates for the interfering waves. Here we call this method the double-array slowness analysis.

~~To investigate the resolution capability of the double-array slowness analysis for the FNET-LAPNET geometry, we make numerical experiments by presuming (a) the same slowness at FNET and LAPNET (4.6 s/deg), and (b) different slownesses at FNET (4.7 s/deg) and LAPNET (4.2 s/deg). The results are plotted in Fig. 5. In both cases, the slownesses of the correlated waves at FNET and LAPNET are well resolved.~~ The results of the double-array slowness analysis for the observed spurious phase are shown in Fig. 5~~6~~a. The azimuths of the correlated waves responsible for the spurious phase are confined to the great-circle direction across FNET and LAPNET, implying that the corresponding microseism noise source should be located on the great circle. The slowness at FNET is distinct from that at LAPNET. The 4.7 s/deg slowness at FNET is valid for deep mantle phases, while the 4.2 s/deg slowness at LAPNET is characteristic of core phases. To investigate the resolution capability of the double-array slowness analysis for the FNET-LAPNET geometry, we make numerical experiments by presuming (a) the same slowness at FNET and LAPNET (4.6 s/deg), and (b) different slownesses at FNET (4.7 s/deg) and LAPNET (4.2 s/deg). Assuming plane waves passing through FNET and LAPNET, the time delays between FNET and LAPNET station pairs can be calculated from Eq. (1). The wavelet of the observed spurious phase (5 to 10 s bandpass filtered) is convolved with the time delays to synthesize the correlation functions. The synthesized correlations are beamed by Eq. (2) for various slownesses. The results are plotted in Fig. 6. In both cases, the slownesses of the correlated waves at FNET and LAPNET are well resolved, ~~Numerical experiments in Fig. 5 have justified~~justifying the reliability of ~~this~~ our slowness discrepancy estimation in Fig. 5a. To investigate if this discrepancy is caused by the lateral heterogeneity of structure beneath the seismic networks, we apply the double-array slowness analysis to the acausal P waves in the FNET-LAPNET correlations as reference (Fig. S4). If lateral heterogeneity causes the slowness discrepancy for the spurious phase, one should also observe a similar phenomenon for the inter-receiver P wave. It is revealed that the slownesses of the interfering waves for the P wave coincide with each other and are close to the predicted value (6.7 s/deg in IASP91 model). The P-wave results again justify the reliability of our slowness estimates, and indicate that lateral heterogeneity is not the reason for the slowness discrepancy observed from ~~Fig. 6~~Fig. 5a.

The peak period of the spurious phase is a typical value for secondary microseisms, which are dominantly excited by ocean wave-wave interactions (Hasselmann, 1963; Longuet-Higgins, 1950). It implies that the noise sources are mainly distributed on the global ocean surface. We propose a slowness-track method to identify the ray paths of the interfering waves from source to receivers that produce the spurious phase (~~Fig. 6~~Fig. 5b). ~~All the body~~Body-wave phases that are discernible in the vertical-component earthquake seismograms are considered as candidates (see labels in Fig. 7). For ~~a specific~~each seismic phase, we compute a distance-traveltime table and a distance-slowness table using the Taup program. ~~the~~The source-receiver distance ~~from source to receiver~~ can be derived from the distance-slowness table,~~.~~ and subsequently, the traveltime can be obtained from the distance-traveltime table. ~~The~~ A pair~~s~~ of seismic phases are rejected if the difference between their source-receiver distances ~~from the source to the receivers~~ differs from the reference FNET-LAPNET distance (63°) or if their time delay deviates from the emerging time of the spurious phase (430 s). For clarity, only several typical P-type phases (P, PcP, PP, and PKP branches) are shown in ~~Fig. 6~~Fig. 5b. Finally, we find that only the correlation between the P wave at FNET and the PKPab wave at LAPNET, emitted from noise source on the great circle ~89° away from FNET and ~152° from LAPNET, can satisfy all the constraints. ~~the correlation between the P wave at ~89° distance and the PKPab wave at ~152° distance is the only combination that satisfies all the constraints.~~ As can be seen from ~~Fig. 6~~Fig. 5b, at 89° distance, the PcP wave arrives almost simultaneously with the P wave, suggesting that PcP-PKPab also has a time delay of ~430 s at 63° inter-receiver distance. However, the PcP slowness (4.1 s/deg) is inconsistent with the estimated 4.7 s/deg slowness at FNET. We ascribe to that PcP is a faint phase, so that signals generated from PcP-PKPab correlations are much weaker than those generated from P-PKPab correlations. The slownesses estimates are crucial for the exclusive determination of the interfering waves. There are also other pairs of seismic phases meeting the constrains other than the slowness estimates. Another example of PcS-PcPPcP correlations that roughly meets the inter-receiver distance (63°) and time delay (430 s), is provided in Fig. S5. The correlated PcS and PcPPcP waves have a common slowness of 3.6 s/deg. The PcS-PcPPcP correlations, as shown by Phạm et al. (2018), may lead to conspicuous signals in coda correlations. However, compared with the direct P and PKP waves in the ambient noise wavefields, the two correlated waves are too weak to have significant contributions to the spurious phase observed in this study. Furthermore, the difference in slowness estimates refutes the PcS-PcPPcP correlation as the dominant term in our case. This example reflects the discrepancies between ambient noise correlations and earthquake coda correlations. ~~The slownesses estimates are crucial for the exclusive determination of the interfering waves.~~

It is logical that the spurious phase is observable in the vertical-vertical noise correlations only, as the correlated waves are both P-type and their amplitudes are dominantly projected onto the vertical components (the lower quality of the horizontal components could be another reason). From ~~Fig. 6~~the receiver locations and source-receiver distances, one can locate the source responsible for the acausal and causal spurious phase, at around [45°S, 174°E] and [12°S, 28°W], respectively. Recall that the spurious phase is not observable in the causal correlations. Comparisons with global oceanic microseism noise sources (Fig. 8) indicate that this time asymmetry can be explained by the difference in the strength of the acausal and causal noise sources: the acausal source in the ocean south of New Zealand is energetic, whereas the causal source in the low-latitude Atlantic east of Brazil is much weaker.

5 Explanation of quasi-stationary phase

The observed spurious phase originates from the correlation between teleseismic P waves and PKPab waves that emanate from the oceanic microseism noise source south of New Zealand. In this section, we explain how such spurious signals can be generated from the interference between waves having distinct slownesses and no common path. Considering ambient noise wavefield as a superposition of waves from uncorrelated sources distributed on Earth's surface (Fig. 9a), the correlation function between the noise records at two receivers is equivalent to a stack of the correlation functions for individual sources (i.e., source averaging; see e.g., Ruigrok et al., 2008). We first simulate the source-wise correlation functions by convolving a wavelet of 6.2 s period with the time delays between the two correlated seismic phases. The final inter-receiver correlation function is obtained from a stack over all sources. In this ray-based simulation, amplitude information is neglected for simplicity. The result for the source averaging of the P-PKPab correlations is shown in Fig. 9b, while that of the P-PKPbc correlations is shown in Fig. 9c for comparison.

The construction of seismic signals from noise correlations has been usually explained with the stationary-phase condition (e.g., Wapenaar et al., 2010). We show such an example in Fig. S4, which is the reconstruction of the inter-receiver P wave from the correlation between the P and PP waves. The P-wave reconstruction is linked to the presence of the extreme (stationary) point on the curve of the P-PP time delay. The P and PP waves from the source at the stationary-phase location (Fig. S4, source A) have a common path and a common slowness. However, as for the spurious phase observed between FNET and LAPNET, the correlated P and PKPab waves have no slowness or ray path in common, and there is no stationary point on the curve of the P-PKPab time delay (Fig. 9b). The strict stationary-phase condition is not fulfilled, and thus the emergence of the spurious phase cannot be explained by this argument. Despite the missing of stationary points on the curve of the P-PKPab time delay, the interference between finite-frequency P and PKPab waves is constructive over the shaded range in Fig. 9b. That leads to the presence of a pulsive signal in the final inter-receiver correlation by source averaging. In contrast to the strict condition of stationary phase, we propose to call this mechanism the condition of quasi-stationary phase, and refer to this range of sources as the quasi-stationary-phase region or effective source region. Recall that the spurious phase has a peak period of 6.2 s. We emphasize that this typical dominant period for secondary microseisms is resultant from the distribution of spectral content of seismic noise sources~~. S~~ — secondary microseisms correspond to the largest peak in the seismic noise spectra (Peterson, 1993).~~At short periods (1 s or shorter),~~ N~~n~~umerical tests of source averaging for the P–PKPab correlations indicate that~~ source averaging for the P-PKPab correlations can still produce signals~~, even at short periods (1 s or less), the spurious phase can be constructed, with narrower effective source region shrinking toward larger source-receiver distances. ~~The concentration of the spectral content of the spurious phase in the band of secondary microseisms is resultant from the distribution of spectral content of seismic noise sources. Secondary microseisms correspond to the largest peak in the seismic noise spectra (Peterson, 1993).~~

Experiences from earthquake observations indicate that PKPbc waves are generally the dominant PKP branch at distances from ~144° (the PKP-wave caustic) to ~153° (Kulhánek, 2002). Microseism studies have also reported that PKPbc waves can be more prominent (e.g., Gerstoft et al., 2008; Landés et al., 2010). However, our analysis reveals that the spurious phase originates from the interference of P waves with PKPab waves, rather than with PKPbc waves. From the source-averaging experiment for the P-PKPbc correlations (Fig. 9c), one can see that the P-PKPbc time delay varies almost linearly against the source-receiver distance, and that the dynamic range of the time delay is broad. Consequently, the signals in the source-wise correlations are out of phase, which leads to a destructive source averaging.

6 Effect of source distribution

The above-described ray-based simulation ~~above~~ is simple to implement and efficient to reveal the origin of the spurious phase. It uses only the phase information and neglects the effect of amplitude variations. This simplification ensures that the spurious phase is not likely to be caused by a strong localized source. To confirm, in this section, we implement a formal wave-based simulation to show that the observed spurious arrivals can be well reproduced under ideally uniform source distribution. As shown in Fig. 8, the spatial variations of the power of global microseism sources are heavily fluctuated. The spurious phase is observable in the acausal correlations because the corresponding source is strong, and is hardly observable in the causal correlations because the responsible source is too weak. It is worth confirming whether the spurious phase can be eliminated with an ideally uniform source distribution or not.

We request the vertical components of the synthetic global broadband seismogram for the *iasp91_2s* model from the IRIS Syngine Data Service (Krischer et al., 2017) powered by the spectral-element program AxiSEM (Nissen-Meyer et al., 2014) and the Python packages Obspy (Krischer et al., 2015) and Instaseis (Van Driel et al., 2015). A mask is applied to the full waveforms (Fig. 10a) to extract the P waves and the PKPab waves (Fig. 10b). Providing that the uncorrelated noise sources are distributed evenly on the global surface, we compute the source-wise correlations and stack them for each inter-station distance, using the data in Fig. 10b. A global section of synthetic P-PKPab correlations is obtained accordingly (Fig. 10c). The spurious phase is clearly reproduced, which suggests that it is not caused by unevenly distributed noise sources.

Repeating the ray-based simulation in Fig. 9b for various inter-receiver distances, one can also obtain a full section of the P-PKPab correlations. Due to the neglect of amplitude information, the ray-based simulation over-estimates the observable range of inter-receiver distances for the spurious phase. The wave-based simulation in this section is undoubtedly more realistic. The theoretical time-distance curve of the spurious phase can be picked from the synthetic sections. It is almost identical for the ray- and wave-based simulations in the observable distance range, and fits well with the observed spurious arrivals in Fig. 4. We also compare the results of the wave-based simulations for two-dimensional plane model (sources along the great circle) and three-dimensional spherical model (sources on global surface). As shown in Fig. S6, the reduction of source dimension leads to an overestimation of the observable distance range of the spurious phase. ~~The picked~~ The time-distance curves picked from the synthetic P-PKPab correlations of two models are ~~the same~~identical in the common distance range, while the amplitudes of signals are different. In the case of uniformly distributed sources, it is safe to implement two-dimensional simulation for efficiency.

7 ~~Discussions and c~~Conclusions

We observe early spurious arrivals in the teleseismic noise correlations between the Japan and Finland stations. These signals are prominent and isolated from other strong seismic phases, making it a good agency to unveil the generation mechanism of such spurious phases. In contrast to previous studies that observed a strong correlation between signal amplitudes and large earthquakes, the spurious signals in this study have no connections to seismicity. We provide evidence in support of that the observed signals origin from the interference between ballistic P waves and PKPab waves that emanate from oceanic microseism noise sources south of New Zealand. The interfering waves have no ray path or slowness in common, and do not meet the traditional condition of stationary phase. The effective source location responsible for the spurious phase does not correspond to a stationary point. We propose a less restrictive condition of quasi-stationary phase, which explains our finite-frequency observations. The strict stationary-phase condition has been used by Phạm et al. (2018) to interpret the spurious phases in the earthquake coda correlations. We expect to see if the quasi-stationary phase arguments can be generalized to the explanation of the coda-derived spurious phases.

The interfering P and PKPab waves have deterministic ray paths that sample the deep mantle and the core. We expect a way to use the spurious phase to investigate the deep Earth structure. The strength of the spurious phase is linked to the power of microseism excitation in a definite, constrained region of noise sources. It is potential to use it to monitor the ocean wave activities and microseism excitations in that specific region. Ambient noise wavefields are dominated by the ballistic waves that persistently emanate from oceanic microseism events, while late coda wavefields after large earthquakes are dominated by highly coherent deep reverberations / high-order core modes separable at intermediate periods of 20 to 50 s (Boué et al., 2014; Maeda et al., 2006; Poli et al., 2017). We appeal to distinguish between global noise correlations and global coda correlations. Multiple spurious arrivals have been observed from the global coda correlation wavefield (Boué et al., 2014; Lin and Tsai, 2013; Phạm et al., 2018). The P-PKPab correlation could not be the unique spurious phase emerging in the global noise correlation wavefield. The double-array slowness analysis and slowness-track method proposed in this paper are also applicable to the analysis of other coda- or noise-derived signals. ~~The spurious phase is definitely linked to the microseism excitations in a constrained region of noise sources. In contrast, noise-derived surface waves are related to sources in a broad stationary-phase region. The stationary-phase regions for the noise-derived P waves are not unique (P-PP, PP-PPP, …). It is potential to monitor the ocean wave activities and microseism excitations in the effective source region with the P-PKPab correlation. The difference in the strength of the spurious phase in the causal and acausal parts of the~~

~~correlation functions is coincident with the difference in the strength of the causal and acausal microseism sources. That testifies the potentiality. The P-PKPab correlation is not the unique spurious phase emerging in global noise correlations. Multiple spurious arrivals can be observed from the global sections of the noise correlations constructed with both real and synthetic seismograms (Boué et al., 2013b, 2014; Ruigrok et al., 2008). The double-array slowness analysis and slowness-track method proposed in this paper are also applicable to other noise-derived seismic signals.~~

Author contribution. LL performed the data processing and designed the synthetic experiments. The code for noise data processing was developed based on an early version by PB. All authors contributed to the analysis of the results. LL prepared the manuscript with contributions from all co-authors. MC wrote the proposal~~provided the funding support~~ leading to this publication.

Competing interests. The authors declare that they have no conflict of interest.

Acknowledgments. The continuous seismograms of FNET and LAPNET were provided by the National Research Institute for Earth Science and Disaster Resilience (http://www.fnet.bosai.go.jp) and the Réseau Sismologique & Géodésique Français (http://www.resif.fr), respectively. The global ~~section of~~ earthquake seismograms were obtained from the IRIS GlobalStacks Data Service (https://ds.iris.edu/ds/products/globalstacks/). The global ~~section of~~ synthetic seismograms were obtained from the IRIS Syngine Data Service (https://ds.iris.edu/ds/products/syngine/). The data of synthetic global microseism noise sources were provided by the IOWAGA products (Rascle and Ardhuin, 2013). The Taup program (Crotwell et al., 1999) and the IASP91 Earth model (Kennett and Engdahl, 1991) were used to calculate the theoretical travel times and ray parameters of seismic phases. The computations were performed with the CIMENT cluster (https://ciment.ujf-grenoble.fr), which is supported by the Rhône-Alpes grant CPER07_13 CIRA (http://www.ci-ra.org). This work is supported by grants from the Simone et Cino Del Duca Foundation, Institut de France, and Labex OSUG@2020 (Investissements d'avenir-ANR10LABX56). The authors ~~also~~ acknowledge the constructive reviews of Pilar Sánchez-Pastor and an anonymous reviewer. We also thank ~~Prof.~~ Sidao Ni for his comments and suggestions on an early draft that improve the manuscript.

References

Allen, R.: Automatic phase pickers: Their present use and future prospects, Bull. Seismol. Soc. Am., 72(6), S225-242, 1982.

Baillard, C., Crawford, W. C., Ballu, V., Hibert, C. and Mangeney, A.: An automatic kurtosis-based P-and S-phase picker designed for local seismic networks, Bull. Seismol. Soc. Am., 104(1), 394–409, doi:10.1785/0120120347, 2014.

Boué, P., Roux, P., Campillo, M. and de Cacqueray, B.: Double beamforming processing in a seismic prospecting context, Geophysics, 78(3), V101–V108, doi:10.1190/geo2012-0364.1, 2013a.

Boué, P., Poli, P., Campillo, M., Pedersen, H., Briand, X. and Roux, P.: Teleseismic correlations of ambient seismic noise for deep global imaging of the Earth, Geophys. J. Int., 194(2), 844–848, doi:10.1093/gji/ggt160, 2013b.

Boué, P., Poli, P., Campillo, M. and Roux, P.: Reverberations, coda waves and ambient noise: Correlations at the global scale and retrieval of the deep phases, Earth Planet. Sci. Lett., 391, 137–145, doi:10.1016/j.epsl.2014.01.047, 2014.

Brenguier, F., Campillo, M., Hadziioannou, C., Shapiro, N. M., Nadeau, R. M. and Larose, E.: Postseismic relaxation along the san andreas fault at parkfield from continuous seismological observations, Science, 321(5895), 1478–1481, doi:10.1126/science.1160943, 2008.

Campillo, M. and Paul, A.: Long-range correlations in the diffuse seismic coda, Science, 299(5606), 547–549, doi:10.1126/science.1078551, 2003.

Campillo, M. and Roux, P.: Crust and lithospheric structure - seismic imaging and monitoring with ambient noise correlations, in Treatise on Geophysics, pp. 391–417., 2015.

Crotwell, H. P., Owens, T. J. and Ritsema, J.: The TauP Toolkit: Flexible seismic travel-time and ray-path utilities, Seismol. Res. Lett., 70(2), 154–160, doi:10.1785/gssrl.70.2.154, 1999.

Van Driel, M., Krischer, L., Stähler, S. C., Hosseini, K. and Nissen-Meyer, T.: Instaseis: Instant global seismograms based on a broadband waveform database, Solid Earth, 6(2), doi:10.5194/se-6-701-2015, 2015.

Gerstoft, P., Shearer, P. M., Harmon, N. and Zhang, J.: Global P, PP, and PKP wave microseisms observed from distant storms, Geophys. Res. Lett., 35(23), 4–9, doi:10.1029/2008GL036111, 2008.

Hasselmann, K.: A statistical analysis of the generation of microseisms, Rev. Geophys., 1(2), 177–210, doi:10.1029/RG001i002p00177, 1963.

Kennett, B. and Engdahl, E. R.: Traveltimes for global earthquake location and phase identification, Geophys. J. Int., 105(2), 429–465, doi:10.1111/j.1365-246X.1991.tb06724.x, 1991.

Krischer, L., Megies, T., Barsch, R., Beyreuther, M., Lecocq, T., Caudron, C. and Wassermann, J.: ObsPy: A bridge for seismology into the scientific Python ecosystem, Comput. Sci. Discov., 8(1), 014003, doi:10.1088/1749-4699/8/1/014003, 2015.

Krischer, L., Hutko, A. R., van Driel, M., Stähler, S., Bahavar, M., Trabant, C. and Nissen-Meyer, T.: On-demand custom broadband synthetic seismograms, Seismol. Res. Lett., 88(4), 1127–1140, doi:10.1785/0220160210, 2017.

Krüger, F., Weber, M., Scherbaum, F. and Schlittenhardt, J.: Double beam analysis of anomalies in the core-mantle boundary region, Geophys. Res. Lett., 20(14), 1475–1478, doi:10.1029/93GL01311, 1993.

Kulhánek, O.: The structure and interpretation of seismograms, in International Geophysics, vol. 81, pp. 333–348, Elsevier B.V., 2002.

Landés, M., Hubans, F., Shapiro, N. M., Paul, A. and Campillo, M.: Origin of deep ocean microseisms by using teleseismic body waves, J. Geophys. Res. Solid Earth, 115(5), 1–14, doi:10.1029/2009JB006918, 2010.

Lin, F. C. and Tsai, V. C.: Seismic interferometry with antipodal station pairs, Geophys. Res. Lett., 40(17), 4609–4613, doi:10.1002/grl.50907, 2013.

Lin, F. C., Tsai, V. C., Schmandt, B., Duputel, Z. and Zhan, Z.: Extracting seismic core phases with array interferometry, Geophys. Res. Lett., 40(6), 1049–1053, doi:10.1002/grl.50237, 2013.

Lobkis, O. I. and Weaver, R. L.: On the emergence of the Green's function in the correlations of a diffuse field, J. Acoust. Soc. Am., 110(6), 3011–3017, doi:10.1121/1.1417528, 2001.

Longuet-Higgins, M. S.: A Theory of the origin of microseisms, Philos. Trans. R. Soc. A Math. Phys. Eng. Sci., 243(857), 1–35, doi:10.1098/rsta.1950.0012, 1950.

Maeda, T., Sato, H. and Ohtake, M.: Constituents of Vertical-component Coda Waves at Long Periods, Pure Appl. Geophys., 163(2–3), 549–566, doi:10.1007/s00024-005-0031-9, 2006.

Nishida, K.: Global propagation of body waves revealed by cross-correlation analysis of seismic hum, Geophys. Res. Lett., 40(9), 1691–1696, doi:10.1002/grl.50269, 2013.

Nissen-Meyer, T., van Driel, M., Stähler, S. C., Hosseini, K., Hempel, S., Auer, L., Colombi, A. and Fournier, A.: AxiSEM: Broadband 3-D seismic wavefields in axisymmetric media, Solid Earth, 5(1), 425–445, doi:10.5194/se-5-425-2014, 2014.

Peterson, J.: Observations and modeling of seismic background noise, U.S. Geol. Surv. Open File Rep. 93-322, (No. 93-322), 1993.

Phạm, T.-S., Tkalčić, H., Sambridge, M. and Kennett, B.: Earth's Correlation Wavefield: Late Coda Correlation, Geophys. Res. Lett., 45(7), 3035–3042, doi:10.1002/2018GL077244, 2018.

Poli, P., Campillo, M. and Pedersen, H.: Body-wave imaging of earth's mantle discontinuities from ambient seismic noise, Science, 338(6110), 1063–1065, doi:10.1126/science.1228194, 2012.

Poli, P., Thomas, C., Campillo, M. and Pedersen, H. A.: Imaging the D″ reflector with noise correlations, Geophys. Res. Lett., 42(1), 60–65, doi:10.1002/2014GL062198, 2015.

Rascle, N. and Ardhuin, F.: A global wave parameter database for geophysical applications. Part 2: Model validation with improved source term parameterization, Ocean Model., 70, 174–188, doi:10.1016/j.ocemod.2012.12.001, 2013.

Rost, S. and Thomas, C.: Array seismology: Methods and applications, Rev. Geophys., 40(3), 1008, doi:10.1029/2000RG000100, 2002.

Roux, P., Cornuelle, B. D., Kuperman, W. a and Hodgkiss, W. S.: The structure of raylike arrivals in a shallow-water waveguide., J. Acoust. Soc. Am., 124(6), 3430–3439, doi:10.1121/1.2996330, 2008.

Ruigrok, E., Draganov, D. and Wapenaar, K.: Global-scale seismic interferometry: Theory and numerical examples, Geophys. Prospect., 56(3), 395–417, doi:10.1111/j.1365-2478.2008.00697.x, 2008.

Sabra, K. G., Gerstoft, P., Roux, P., Kuperman, W. A. and Fehler, M. C.: Surface wave tomography from microseisms in Southern California, Geophys. Res. Lett., 32(14), 1–4, doi:10.1029/2005GL023155, 2005.

Saragiotis, C. D., Hadjileontiadis, L. J. and Panas, S. M.: PAI-S/K: A robust automatic seismic P phase arrival identification scheme, IEEE Trans. Geosci. Remote Sens., 40(6), 1395–1404, doi:10.1109/TGRS.2002.800438, 2002.

Shapiro, N. M. and Campillo, M.: Emergence of broadband Rayleigh waves from correlations of the ambient seismic noise, Geophys. Res. Lett., 31(7), 8–11, doi:10.1029/2004GL019491, 2004.

Shapiro, N. M. N., Campillo, M. and Stehly, L.: High-resolution surface-wave tomography from ambient seismic noise, Scienc, 307(5715), 1615–1618, doi:10.1126/science.1108339, 2005.

Spica, Z., Perton, M. and Beroza, G. C.: Lateral heterogeneity imaged by small-aperture ScS retrieval from the ambient seismic field, Geophys. Res. Lett., 44(16), 8276–8284, doi:10.1002/2017GL073230, 2017.

Tkalčić, H. and Phạm, T.-S.: Shear properties of Earth's inner core constrained by a detection of J waves in global correlation wavefield, Science (80)., 362(6412), 329–332, doi:10.1126/science.aau7649, 2018.

Wang, T. and Song, X.: Support for equatorial anisotropy of Earth's inner-inner core from seismic interferometry at low latitudes, Phys. Earth Planet. Inter., 276, 247–257, doi:10.1016/j.pepi.2017.03.004, 2017.

Wang, T., Song, X. and Xia, H. H.: Equatorial anisotropy in the inner part of Earth's inner core from autocorrelation of earthquake coda, Nat. Geosci., 8(February), 1–4, doi:10.1038/NGEO2354, 2015.

Wapenaar, K.: Retrieving the elastodynamic Green's function of an arbitrary inhomogeneous medium by cross correlation, Phys. Rev. Lett., 93(25), 254301, doi:10.1103/PhysRevLett.93.254301, 2004.

Wapenaar, K., Draganov, D., Snieder, R., Campman, X. and Verdel, A.: Tutorial on seismic interferometry: Part 1 — Basic principles and applications, Geophysics, 75(5), 75A195-75A209, doi:10.1190/1.3457445, 2010.

Wegler, U., Nakahara, H., Sens-Schönfelder, C., Korn, M. and Shiomi, K.: Sudden drop of seismic velocity after the 2004 Mw6.6 mid-Niigata earthquake, Japan, observed with Passive Image Interferometry, J. Geophys. Res. Solid Earth, 114(6), B06305, doi:10.1029/2008JB005869, 2009.

Westfall, P. H.: Kurtosis as Peakedness, 1905–2014. R.I.P., Am. Stat., 68(3), 191–195, doi:10.1080/00031305.2014.917055, 2014.

Xia, H. H., Song, X. and Wang, T.: Extraction of triplicated PKP phases from noise correlations, Geophys. J. Int., 205(1), 499–508, doi:10.1093/gji/ggw015, 2016.

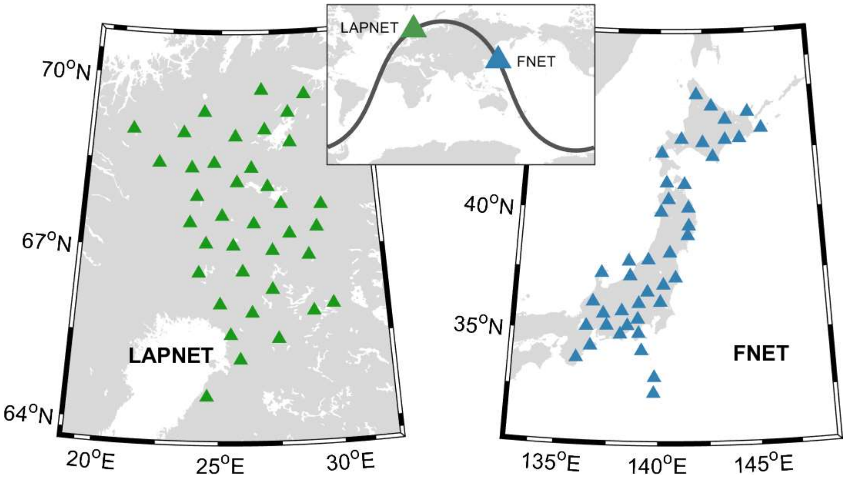

Figure 1: Geographic locations of the 38 stations of the LAPNET array in Finland and the 41 stations of the FNET array in Japan.

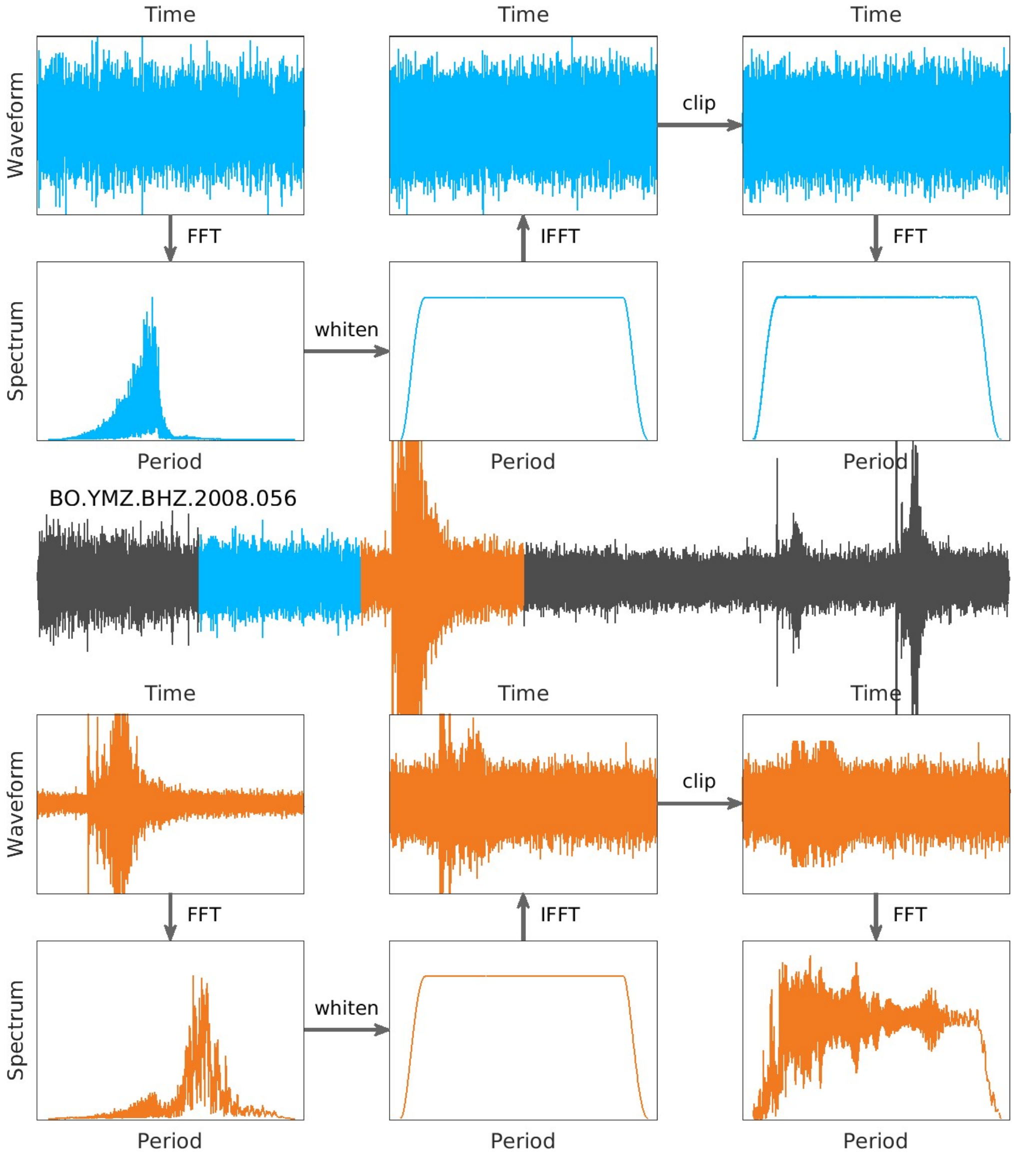

Figure 2: Examples of segment-based noise data processing. A segment with stationary noise and a segment containing a M7.2 teleseism from a daily trace recorded by FNET station BO.YMZ are used for demonstration.

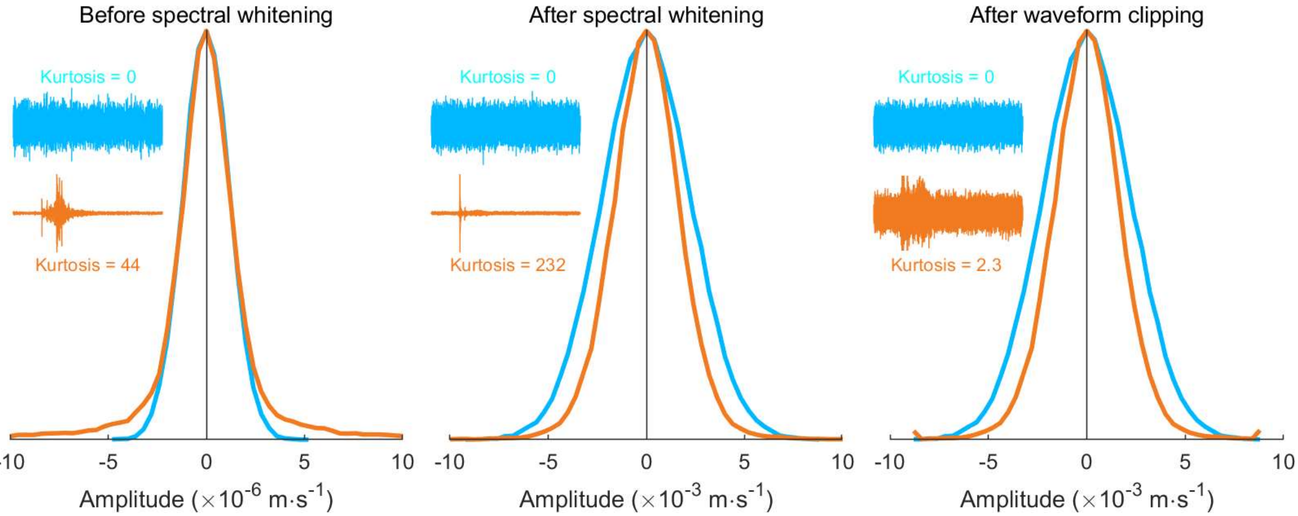

Figure 3: Kurtosis-based selection filter to determine if a segment contains large-amplitude transients. The two segments used here are the same as in Fig. 2. For display, waveforms are plotted in varying scales. The amplitude histograms are normalized by their own maximums. Histogram tails outside the horizontal axis limits are cropped.

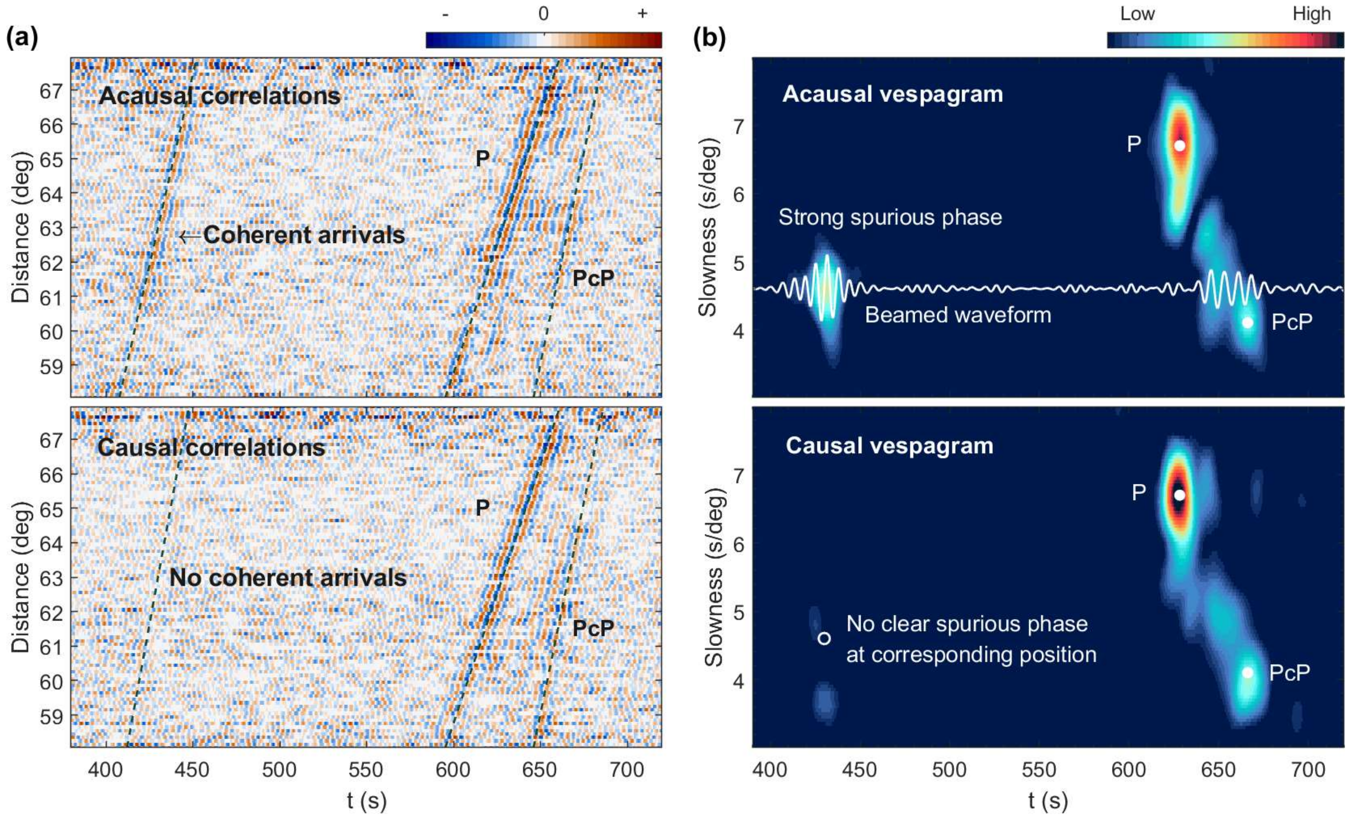

Figure 4: (a) Waveform sections and (b) vespagrams of the acausal and causal parts of the vertical-vertical noise correlations filtered in the period band from 5 s to 10 s. The acausal section for negative time lags is flipped to share a common time axis with the causal section.

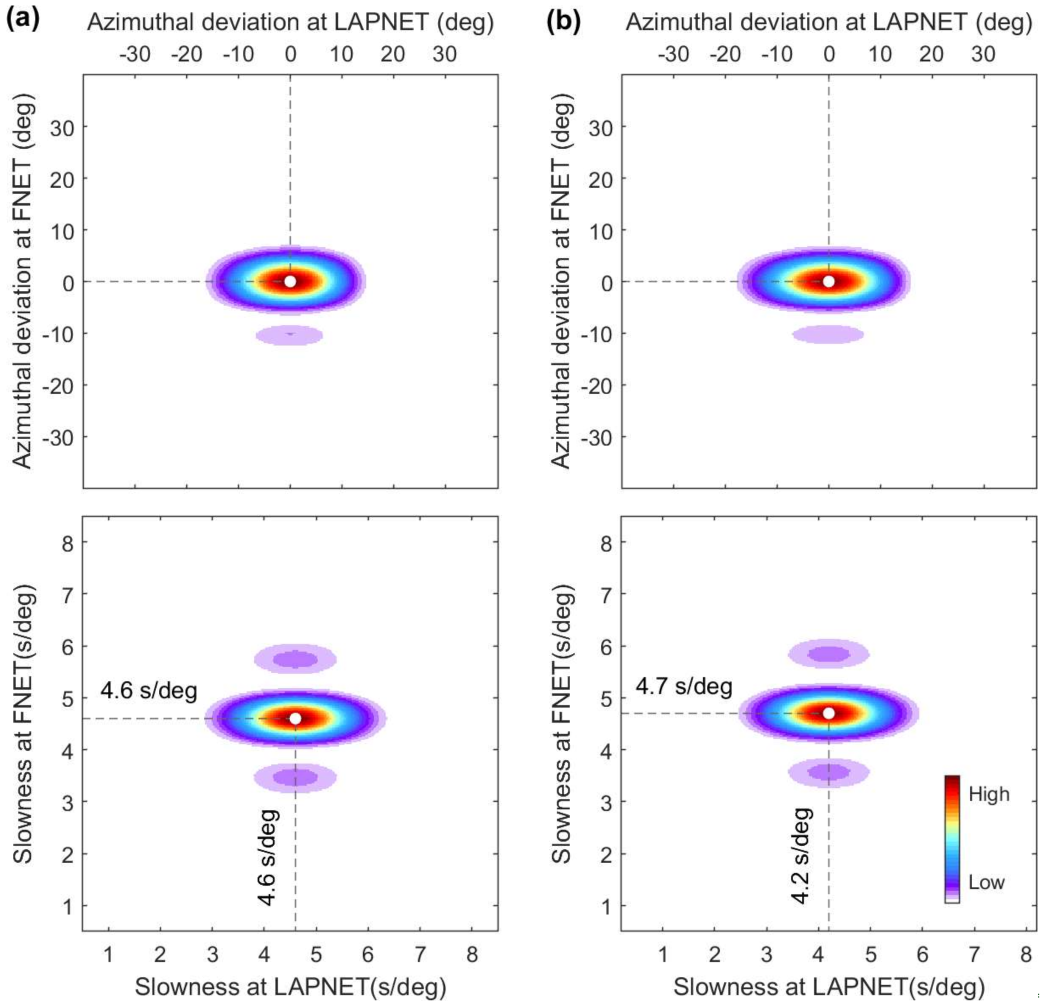

~~**Figure 5: Numerical tests for the double-array slowness analysis of the FNET-LAPNET correlations at a seismic period of 6.2 s. The input azimuths of the interfering waves are confined to the great circle crossing FNET and LAPNET. The azimuthal deviation refers to the clockwise azimuthal deviation of slowness from the great circle. The input slownesses of the interfering waves are (a) 4.6 s/deg at both LAPNET and FNET and (b) 4.2 s/deg at LAPNET and 4.7 s/deg at FNET, which are well resolved by the slowness analysis.**~~

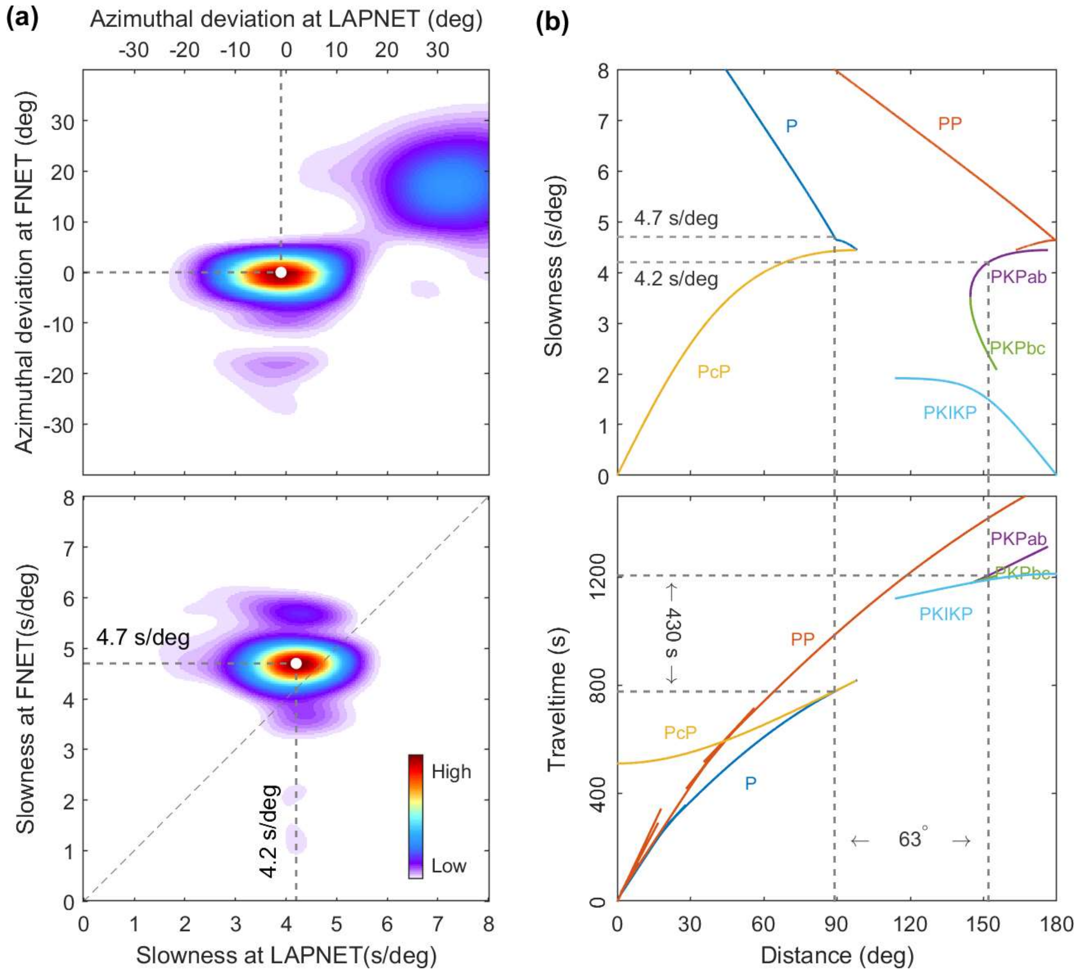

Figure ~~6~~5: (a) Results of the double-array slowness analysis for the observed spurious phase. (b) Tracking the interfering waves responsible for the spurious phase using the slowness estimates.

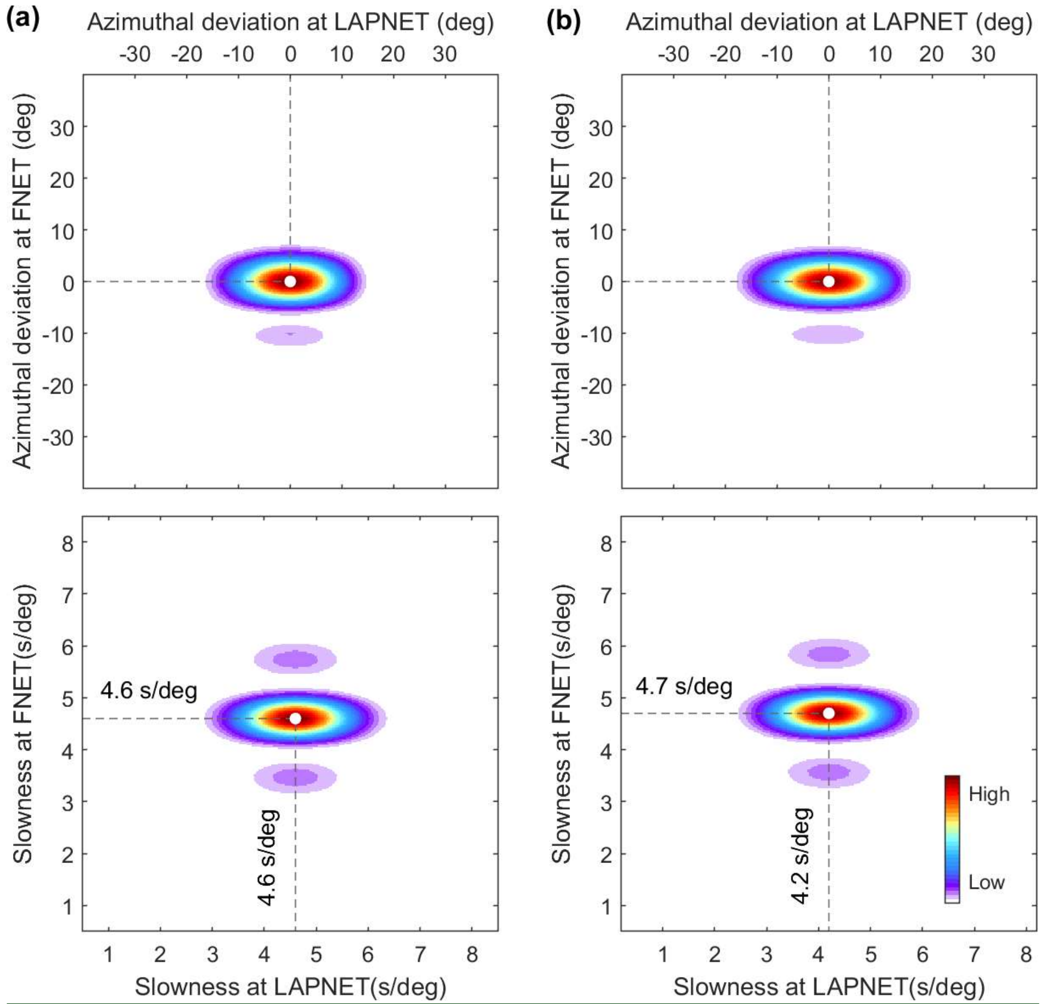

Figure 65: Numerical tests for the double-array slowness analysis of the FNET-LAPNET correlations at a seismic period of 6.2 s. The input azimuths of the interfering waves are confined to the great circle crossing FNET and LAPNET. The azimuthal deviation refers to the clockwise azimuthal deviation of slowness from the great circle. The input slownesses of the interfering waves are (a) 4.6 s/deg at both LAPNET and FNET and (b) 4.2 s/deg at LAPNET and 4.7 s/deg at FNET, which are well resolved by the slowness analysis.

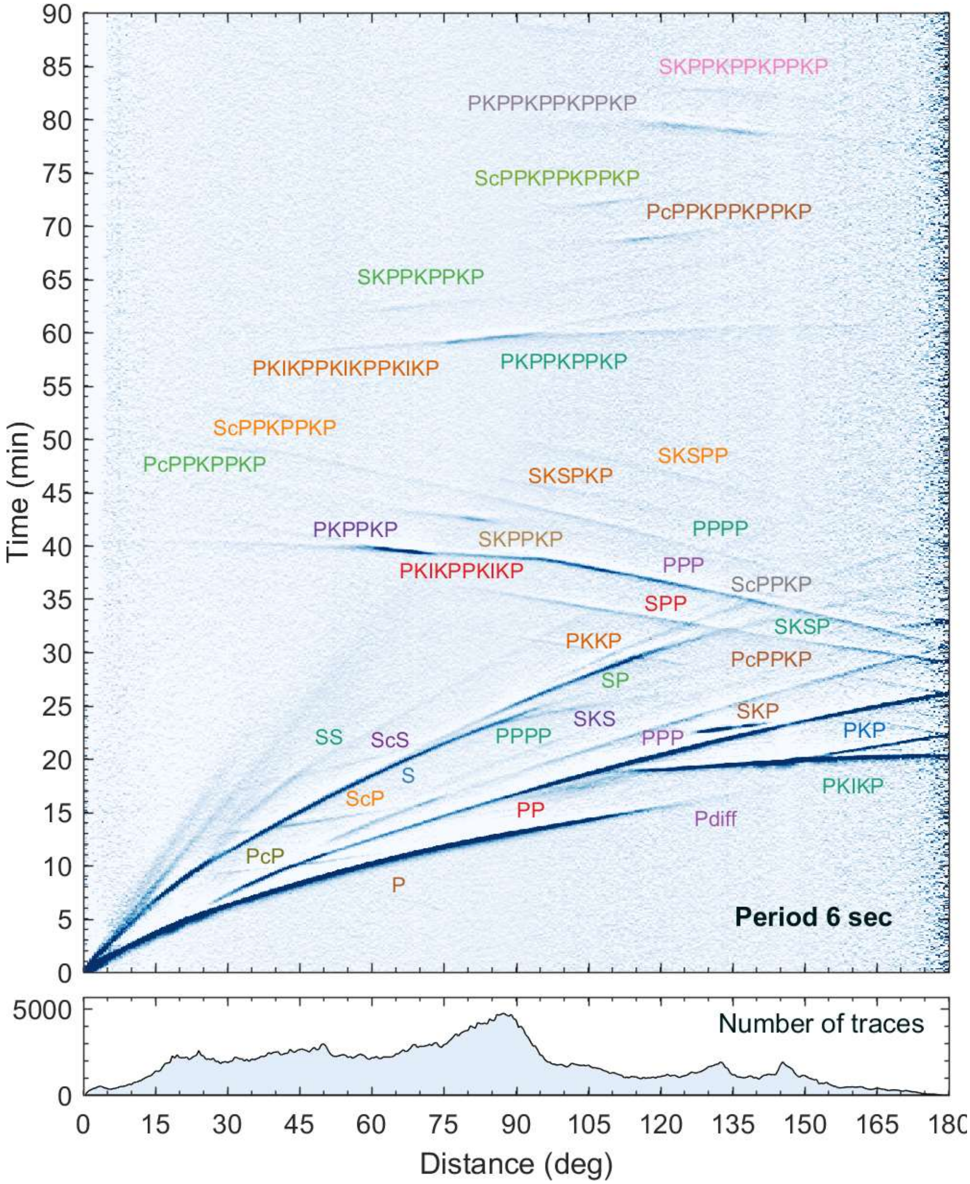

Figure 7: **Global stacks of the vertical components of the seismograms selected from over 2,500 shallow earthquakes (event depth ≤ 50 km and magnitude ≥ 5.4) occurring between 1995 and 2013. The seismograms are filtered around 6 s period and converted into traces of STA/LTA ratios. The STA/LTA traces are binned by epicentral distances in an interval of 0.5° and normalized for plotting. More details can be found on the IRIS Data Services Products website.**

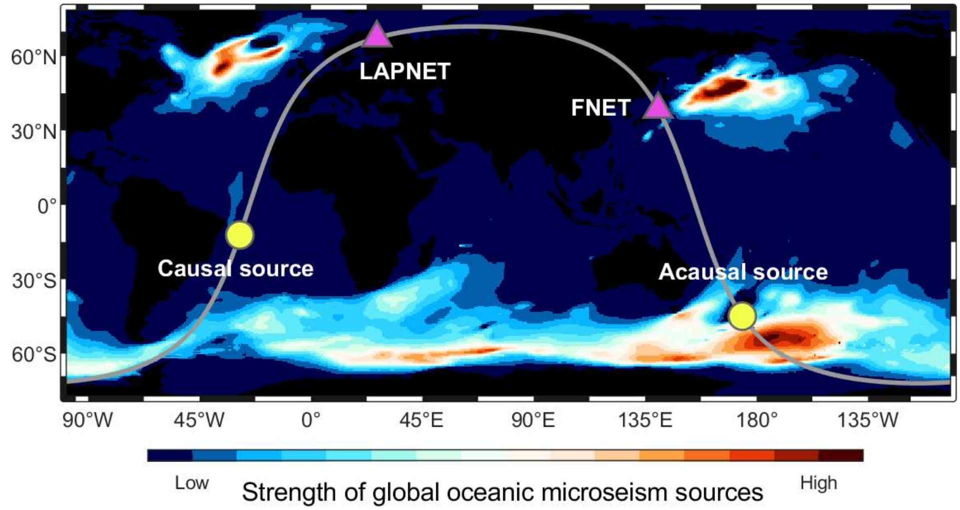

Figure 8: The global map of oceanic microseism excitation in 2008, at a seismic period of 6.2 s (Rascle and Ardhuin, 2013). The source responsible for the acausal spurious phase is located in the ocean south of New Zealand.

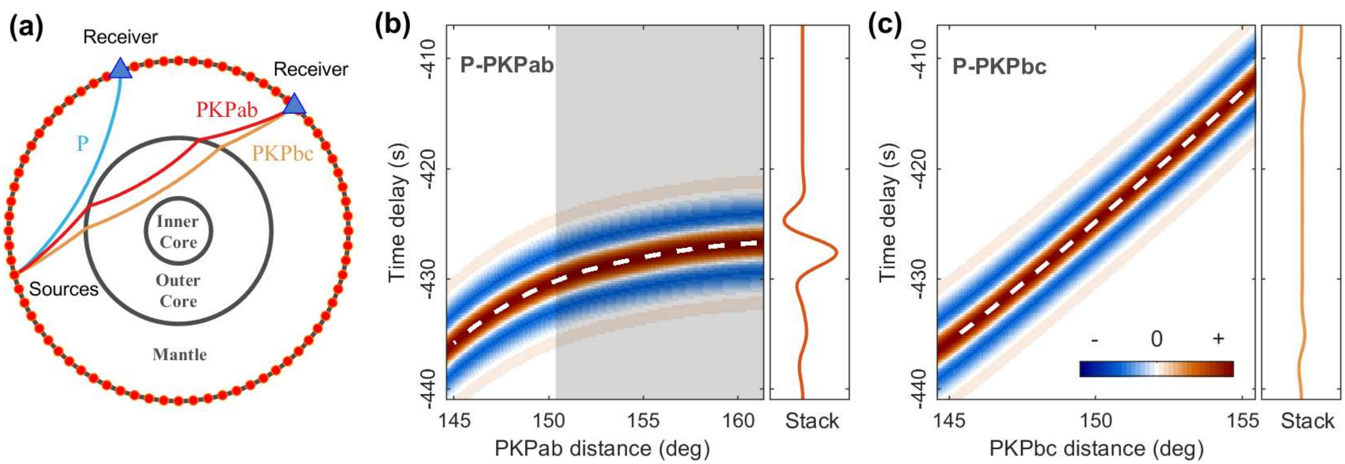

Figure 9: (a) Geometry of the model to synthesize the inter-receiver correlation function of teleseismic P and PKP waves via source averaging. (b) Source-averaging experiment for the P-PKPab correlations at an inter-receiver distance of 63°. The source-wise P-PKPab correlation functions are synthesized by convolving a 6.2 s period wavelet with the P-PKPab time delays. The final inter-receiver correlation function is obtained by stacking the source-wise correlations. (c) Source-averaging experiment for the P-PKPbc correlations.

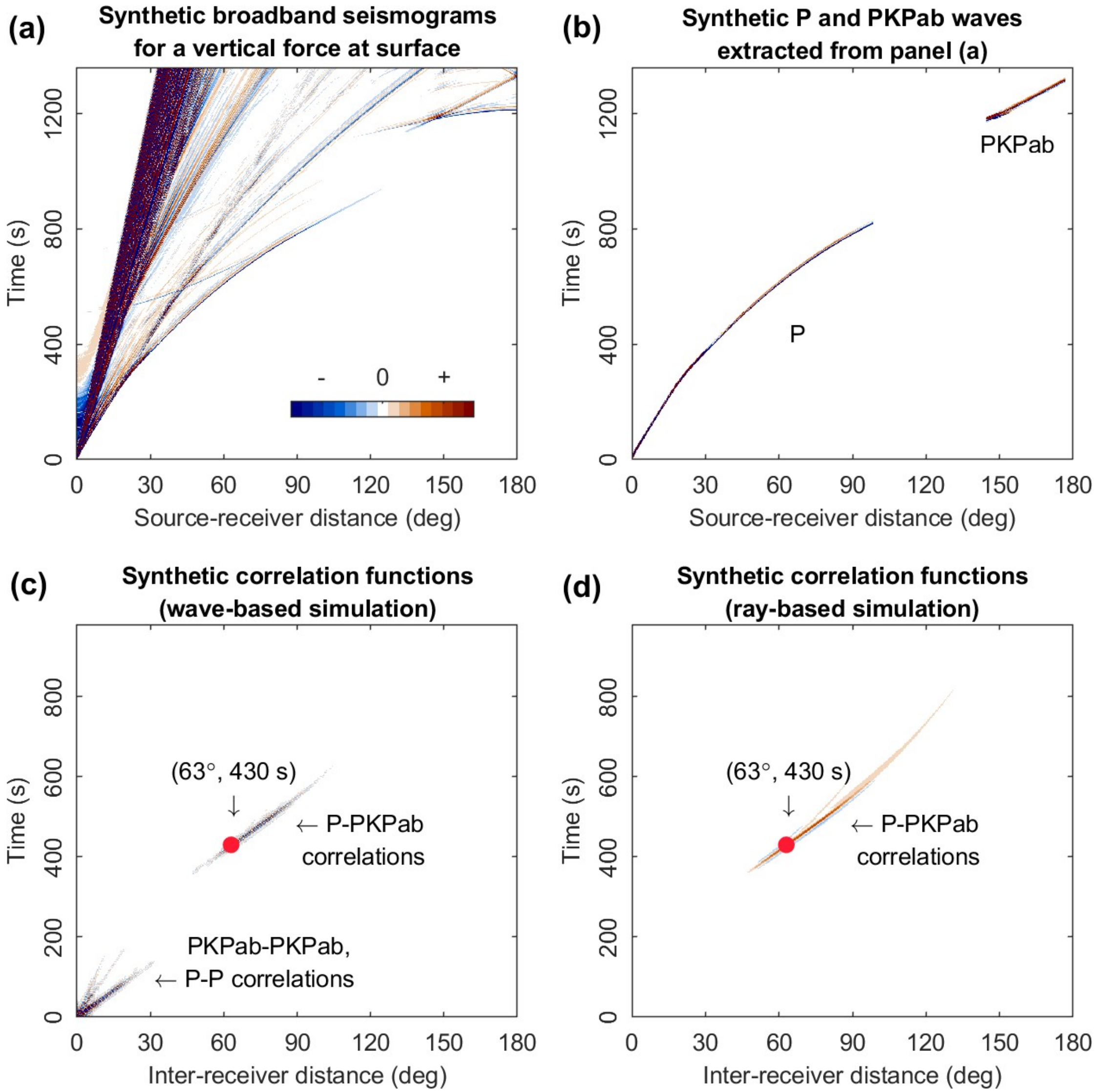

Figure 10: (a) Global section of synthetic broadband (2 s to 100 s) seismograms obtained from the IRIS Syngine Data Service. (b) Seismograms containing P and PKPab waves only, by muting other seismic phases in (a). (c) Global section of inter-receiver correlations using the waveform data in (b). (d) Global section of synthetic P-PKPab correlations using the ray-based method in Fig. 9.